International Journal of Nanomedicine

Dovepress
open access to scientific and medical research

Open Access Full Text Article

ORIGINAL RESEARCH

Design and Application of pH-Responsive Liposomes for Site-Specific Delivery of Cytotoxin from *Cobra Venom*

Qing Lin[1,2,*], Yafei Jing[2,3,*], Cailing Yan[2], Xinyi Chen[2], Qiong Zhang[2], Xinhua Lin[2,3], Yunlu Xu[2,4], Bing Chen[2,3]

[1]Department of Pharmacy, Affiliated Fuzhou First Hospital of Fujian Medical University, Fujian Medical University, Fuzhou, Fujian, People's Republic of China; [2]School of Pharmacy, Fujian Medical University, Fujian, People's Republic of China; [3]Key Laboratory of Nanomedical Technology (Education Department of Fujian Province), Fujian Medical University, Fuzhou, Fujian, People's Republic of China; [4]Center of Translational Hematology, Fujian Medical University Union Hospital, Fujian Medical University, Fuzhou, Fujian, People's Republic of China

*These authors contributed equally to this work

Correspondence: Bing Chen, School of Pharmacy, Fujian Medical University, Fuzhou, 350122, People's Republic of China, Email BingChen_001@126.com; BingChen_001@fjmu.edu.cn; Yunlu Xu, Center of Translational Hematology, Fujian Medical University Union Hospital, Fujian Medical University, Fuzhou, 350122, People's Republic of China, Email xuyunlu3578@126.com

Background: Current immunotherapies with unexpected severe side effects and treatment resistance have not resulted in the desired outcomes for patients with melanoma, and there is a need to discover more effective medications. Cytotoxin (CTX) from *Cobra Venom* has been established to have favorable cytolytic activity and antitumor efficacy and is regarded as a promising novel anticancer agent. However, amphiphilic CTX with excellent anionic phosphatidylserine lipid-binding ability may also damage normal cells.

Methods: We developed pH-responsive liposomes with a high CTX load (CTX@PSL) for targeted acidic-stimuli release of drugs in the tumor microenvironment. The morphology, size, zeta potential, drug-release kinetics, and preservation stability were characterized. Cell uptake, apoptosis-promoting effects, and cytotoxicity were assessed using MTT assay and flow cytometry. Finally, the tissue distribution and antitumor effects of CTX@PSL were systematically assessed using an in vivo imaging system.

Results: CTX@PSL exhibited high drug entrapment efficiency, drug loading, stability, and a rapid release profile under acidic conditions. These nanoparticles, irregularly spherical in shape and small in size, can effectively accumulate at tumor sites (six times higher than free CTX) and are rapidly internalized into cancer cells (2.5-fold higher cell uptake efficiency). CTX@PSL displayed significantly stronger cytotoxicity (IC_{50} 0.25 μg/mL) and increased apoptosis in than the other formulations (apoptosis rate 71.78 ±1.70%). CTX@PSL showed considerably better tumor inhibition efficacy than free CTX or conventional liposomes (tumor inhibition rate 79.78±5.93%).

Conclusion: Our results suggest that CTX@PSL improves tumor-site accumulation and intracellular uptake for sustained and targeted CTX release. By combining the advantages of CTX and stimuli-responsive nanotechnology, the novel CTX@PSL nanoformulation is a promising therapeutic candidate for cancer treatment.

Keywords: cobra venom cytotoxin, tumor microenvironment, pH-responsive, targeted delivery, liposomes

Introduction

Correct diagnosis and early intervention is crucial for successful treatment of melanoma. Most malignant and highly aggressive melanoma have a high mortality rate if the opportunity for early surgical treatment is missed.[1] It is estimated that deaths due to malignant melanoma will increase by about 68% with 510,000 new cases diagnosed (approximately 50% increase) globally by the year 2040.[2] The recent development of immunotherapies and targeted therapies has brought hope to patients with malignant melanoma. However, low treatment response rates, unexpected side effects, and

Received: 31 January 2024
Accepted: 25 May 2024
Published: 6 June 2024

treatment resistance have limited their widespread use and popularity.[3,4] Therefore, there is an urgent need to develop new drugs to improve the efficacy of melanoma treatment.

Cytotoxins (CTX) from *cobra venom* are polypeptides of 60–63 amino acid residues (relative molecular weight ~6–7 kDa, pI ≥ 10), which are key components in the venom responsible for pharmacological activity.[5,6] CTX exhibit amphiphilic properties and belong to the three-finger toxin superfamily, which can translocate to the intermembrane space to affect the integrity of lipid membranes and influence the structure and function of membrane proteins.[7–9] Previous studies have confirmed that CTX possesses a remarkable ability to induce apoptosis, necrosis, and oncolysis by activating mitochondrial and/or lysosomal cell death-associated signaling cascades.[10,11] Based on promising results from preclinical studies, three drug candidates derived from snake venom (ATN-161, GLPG0187, and vicrostatin) are currently undergoing clinical Phase I or II trials as potential antitumor agents, including breast cancer, ovarian carcinoma, and malignant melanoma.[12–14] However, Patients who receive high-dose intravenous injections of CTX often experience local injection area tissue necrosis or systemic neurotoxicity, severely limiting their clinical potential.[15,16] Therefore, there is an urgent need to establish an efficient strategy to ameliorate normal tissue damage and modulate focal CTX concentrations within the therapeutic window.

Nanotechnology has the potential to revolutionize the field of drug delivery and can be designed to improve the efficacy and safety of drug delivery systems by allowing site-specific targeted delivery, controlled release, and improved bioavailability of drugs.[17–21] Among the various drug delivery systems, liposomes are the most popular and represent advanced and versatile nanotechnology. They not only have excellent potential for modification and functionalization, but can also encapsulate a wide range of drugs while demonstrating biocompatibility and non-immunogenicity.[22,23] Additionally, liposomes are economical, easily fabricated, and acceptable for clinical use.[24] Nevertheless, common liposome formulations have obvious defects in terms of slow drug release profiles and a lack of fusion promotion activity after internalization into the endosomal compartment.[25] Recent advances have given more attention to stimuli-sensitive drug delivery systems based on tumor microenvironment (TME) characteristics that can maintain long-term circulating stability and preferentially accumulate and respond to release drugs at the tumor site.[26–28]

Malignant melanoma is a highly heterogeneous disease, and TME is composed of fibroblasts, mesenchymal cells, and extracellular matrix components that play important roles in the growth, invasion, and metastasis of tumor cells.[29,30] Melanoma cells rewire their metabolism to rapidly proliferate and survive, resulting in lactic acid accumulation and a weakly acidic (pH 6.5 ~ 6.8) tumor environment.[31] PH-responsive nanoliposomes can take advantage of the acidic nature of TME, which can be a promising strategy for improving antimelanoma efficacy and reducing toxic side effects through CTX-targeted accumulation and sustained release via tumor site-specific delivery.[32–35]

Therefore, we constructed pH-sensitive liposomes aiming to enhance CTX accumulation and release at the tumor site based on melanoma's microenvironment characteristics, while also holding promising clinical translational value. We measured the morphology, particle size, encapsulation efficiency, drug loading and stability of CTX@PSL. Moreover, we systematically evaluated the pH-stimuli release properties, cellular uptake behaviors, and cancer cell death profiles in vitro, as well as tissue distribution, antitumor efficacy, and toxicity in vivo using a B16-F10 xenograft mouse model. We hypothesized that: (1) CTX@PSL, which are uniformly distributed and regularly spherical with approximately 100 nm the large size, could evade phagocytosis by the reticuloendothelial system (RES); (2) CTX@PSL enter and accumulate in the tumor tissue through enhanced permeability and retention (EPR) effect; (3) pH response CTX release and achieve precise therapy, improve efficacy and reduce adverse reactions.

Materials and Methods

Materials

Cholesteryl hemisuccinate (CHEMS) and distearoylphosphatidylethanolamine polyethylene glycol 2000 (mPEG2000-DSPE) were obtained from Avanti Polar Lipids (Alabaster, Alabama, USA). Dioleoyl phosphatidylethanolamine (DOPE)

and distearoyl phosphatidylcholine (DSPC) were purchased from AVT Pharmaceutical Tech Co., Ltd (Shanghai, China). Cholesterol and soy lecithin were obtained from Aladdin (Shanghai, China). Cobra venom cytotoxin (CTX) was provided by the Snake-Venom Research Institute of Fujian Medical University (Fujian, China). RPIM-1640, PBS buffer, trypsin, and penicillin-streptomycin were obtained from HyClone (Logan, Utah, USA). The fetal bovine serum was purchased from Herui Biotechnology (Fujian, China). Other chemicals and reagents were acquired from Sinopharm Chemical Reagent Corporation. (Shanghai, China).

Preparation of Cobra Venom Cytotoxin Loaded pH-Sensitive Liposomes (CTX@PSL)

Liposomal nanoparticles loaded with CTX were synthesized using a thin-film hydration technique.[35] The principal preparation process can be briefly summarized as follows: DOPE, CHEMS, DSPC, and mPEG2000-DSPE (32:8:34:5, w/w) were dissolved in chloroform and then evaporated in a rotary vacuum system at 40 °C to obtain a thin film. Complete evaporation was achieved by applying a rotary vacuum pump for at least 30 min. Next, PBS containing CTX (sample concentration 5.7563 mg/mL) was added to the above liposome solution with the ratio of lipids to CTX fixed at 5:1 (w/w). Rotary evaporation at 40 °C was continued for 30 min to obtain CTX@PSL.

CTX@PSL was ultrasonically dispersed for 5 min and downsized using a small extruder (Avanti Polar Lipids, Alabaster, AL), each through a polycarbonate membrane with 200 nm pores and 100 nm pores 5 times.[36] In order to remove unencapsulated CTX, the liposomes were placed in a regenerated cellulose membrane tube (MWCO 50 kDa), then dialyzed against PBS buffer for 24 h under stirring at 4 °C. pH-sensitive classical liposomes containing CTX (CTX@Lips) were prepared similarly.

Liposome Characterization

The morphological characteristics of CTX@PSL were observed by transmission electron microscopy (TEM) (Tecnai G2, FEI, USA). After diluting the samples with pure water (pH 7.0), the particle size (PS), polydispersity index (PDI) and surface zeta potential (ξ) of liposomes were measured by using dynamic light scattering (DLS) (Litesizer 500, Anton Paar, Austria).

The prepared liposomes were stored at 4 °C to evaluate their stability. Changes in PS, PDI, and encapsulation efficiency (EE) were measured on days 1, 7, 15, and 30 after the preparation.

Drug loading (DL) is the weight percentage of drug in the liposome prescription. The liposome encapsulation efficiency (EE) was determined using cryogenic ultrafiltration centrifugation. A 50 μL aliquot of liposomal suspension was dissolved in 200 μL of 5% sodium dodecyl sulfate (SDS) to lyse the liposomes and release the CTX. Another 50 μL of liposome suspension was diluted with 200 μL of PBS buffer and then centrifuged to the filtrate. The concentrations of total CTX added (C_{total}) and unencapsulated CTX ($C_{unloaded}$) were determined using a BCA protein concentration assay kit (Beyotime Biotechnology Co., Ltd., Shanghai, China) according to the guidelines provided by the manufacturer. The EE is expressed by:

$$EE\ (\%) = \left(1 - \frac{C_{unloaded}}{C_{total}}\right) \times 100\%$$

In vitro Release Study

The release of CTX was investigated by thermostatic shock dialysis. Three equal volumes of CTX@PSL solution were placed in regenerated cellulose dialysis bags (Yanaye Bio-Technology Co., Ltd., China, MWCO 50 kDa). The dialysis bags were sealed and placed in PBS release media at pH 5.5, 6.5 and 7.4, then shaken at 37 °C and 100 r/min to release CTX from liposomes. Samples were collected and supplemented with fresh release media of the same pH at various time intervals. The CTX concentration was measured using a BCA protein concentration assay kit to calculate the release rate and to plot the release curve.

Cell Uptake Efficiency

To monitor the intracellular delivery of CTXs, CTX was labeled with the vivo Tag™ 680XL Protein Labeling Kit (PerkinElmer, USA) according to the instructions of the NIR Fluorochrome Labeling Kit. Fluorescent-labeled CTX (Dir@CTX) was encapsulated in different Materials to synthesize liposomes.

The mouse melanoma cell line B16-F10 used for the in vitro assays was obtained from the Biological Research Institute of the Chinese Academy of Sciences (Shanghai, China). Cells were cultured in RPMI-1640 containing 10% fetal bovine serum (FBS) and 1% penicillin-streptomycin at 37 °C in a humidified standard incubator with 5% CO_2 atmosphere. B16-F10 cells were inoculated into a 96-well plate at a density of 4×10^5 cells per well and incubated for 24 h. After treatment with fluorescently labeled liposomes Dir@CTX, Dir@CTX@Lips, and Dir@CTX@PSL (CTX concentration: 1 μg/mL), they were incubated further for 0.5, 3, and 6 h. All cells in each well were collected and analyzed with FACSVerse™ flow cytometer (excitation wavelength: 668 nm, Becton Dickinson, USA). The intracellular fluorescence intensity of Dir@CTX was quantified using FlowJo V10 software (Becton Dickinson, USA).

Flow Cytometry Analysis of Apoptosis

To investigate the cell death caused by CTX@PSL, B16-F10 cells were analyzed by flow cytometry after Annexin V-FITC/PI staining. All fluorescent cells were quantified using FACSVerse™ flow cytometer and subsequently analyzed using FlowJo V10.

B16-F10 cells were inoculated on 6-well cell culture plates, treated with CTX, CTX@Lips, and CTX@PSL (CTX concentration: 0.5 μg/mL), and incubated for 24 h. The cells were then trypsinized and collected, including all suspended and adherent cells, in the well. 5 μL Annexin V-FITC and 10 μL PI were added to 1×10^5 cells for 15 min at room temperature in the dark. The cells were immediately analyzed with flow cytometry.

In vitro Cytotoxicity Assay

The inhibitory effect of CTX and its nano-formulation on B16-F10 cells was assessed using MTT assay. For further comparison, we replaced pH-sensitive membrane material CHEMS with pH-insensitive cholesterol to prepare classical cytotoxin- loaded liposomes without pH sensitivity (CTX@Lips). 1×10^4 B16-F10 cells per well were inoculated into a 96-well plate and cultured for 24 h. Following cell adhesion and growth, the medium in the 96-well plate was replaced with different concentrations of CTX@PSL, CTX@Lips, and CTX diluted with complete medium and incubation continued for 24 h. Then, 20 μL of MTT solution (5 mg/mL) was added to each well and allowed to stand for 4 h. Subsequently, the medium with MTT was replaced with 150 μL DMSO to dissolve the formazan crystals. The absorbance was measured at 490 nm with an ELISA plate reader (Thermo Fisher, USA), and the cell inhibition was calculated according to the following formula.

$$Cell\ inhibition\ (\%) = \left(1 - \frac{OD_{sample} - OD_{blank}}{OD_{control} - OD_{blank}}\right) \times 100\%$$

Dose- response curves were plotted using GraphPad Prism software (San Diego, CA, USA) and IC_{50} was calculated.

In vivo Fluorescence Imaging Study

All animal experiments were approved by the Laboratory Animal Ethics Committee of Fujian Medical University and were conducted in accordance with the National Institute Guide for the Care and Use of Laboratory Animals.

A mouse melanoma model was established by subcutaneous injection of 1×10^6 B16-F10 cells into the right axilla of ICR mice. When the average tumor volume reached approximately $1000mm^3$, the mice were randomly divided into two groups.

To evaluate the tumor targeting ability and drug distribution of CTX@PSL, liposomes were reassembled using fluorescent protein-labeled CTX to track the distribution of liposomes. Mice were injected with Dir@CTX and Dir@CTX@PSL via the tail vein at a CTX dose of 0.6 mg/kg per mouse. At 0.5, 2, and 6 h after administration, the mice were sacrificed and the liver, kidney, lung, spleen, heart, and tumor tissues were collected for

fluorescence imaging. IVIS small animal optical imaging system (IVIS®Spectrum, PerkinElmer, USA) was used to perform fluorescence imaging to observe the in vivo targeted distribution of Dir@CTX.

Antitumor Study in a Melanoma Mouse Model

The melanoma mouse model was established as described above and the mice were randomly divided into three groups of 10 mice each. Physiological saline, CTX, and CTX@PSL were injected intraperitoneally once daily for 13 days.

Group 1: negative control (received physiological saline).

Group 2: CTX (dose equivalent to 0.6 mg/kg CTX).

Group 3: CTX@PSL (dose equivalent to 0.6 mg/kg CTX).

Weight Monitoring and Tumor Weight Comparison

During the experiment, the animals were observed for appearance, activity, feeding, and weight change (on days 0, 3, 7, 10, and 13). On day 14, the mice were euthanized, and the tumor tissue was weighed to calculate the tumor growth inhibition rate (IR).

$$IR\ (\%) = \left(1 - \frac{M_{sample}}{M_{control}}\right) \times 100\%$$

Histopathological Assessment

After euthanasia, livers, kidneys, lungs, spleens and hearts were harvested, fixed in neutral buffered formaldehyde (10%), placed in paraffin blocks, and sectioned. Subsequently, the tissues were stained with hematoxylin and eosin (H&E) and observed under a light microscope (Nikon, Tokyo, Japan) with a digital camera attached to assess the damage on the tissues.[37]

Statistical Methods

Statistical analysis was performed with GraphPad Prism software. The data obtained were expressed as mean ± standard deviation (SD). Student's *t*-test was used for comparison between two groups. ANOVA was used for multiple comparisons. And $P<0.05$ was regarded as statistically significant difference.

Results and Discussion

Liposomes are high-quality targeted nanocarriers for antitumor drugs. Since the FDA approved the first liposome formulation of adriamycin hydrochloride (Doxil) for marketing, liposomes have been widely used as new dosage forms for biopharmaceutical products.[38]

Cobra venom cytotoxin induces apoptosis in tumor cells by altering the mitochondrial membrane potential, releasing cytochrome C, activating caspase 9 and caspase 3, or by increasing the permeability of the lysosomal membrane, leading to the release of proteases from lysosomes into the cytoplasm.[39,40] Furthermore, the TME (pH: 6.5 ~ 6.8) and tumor cell endosomes (pH: 4.5 ~ 5.5) are acidic and have a pH gradient difference from normal cells (pH: 7.2 ~ 7.5).[32,33] Based on this characteristic, we combined cobra venom cytotoxin (CTX) with nanoliposomes for targeted delivery, it is a novel strategy for CTX in clinical applications.

Generally, pH-responsive nanoparticles are fabricated using acid-sensitive chemical bonds or ionizable moieties.[35,41,42] In this study, we selected dioleoyl phosphatidylethanolamine (DOPE) and cholesteryl hemisuccinate (CHEMS) as pH-sensitive responsive materials and modified distearoyl phosphatidylethanolamine-polyethylene glycol 2000 (mPEG2000-DSPE) in the shell to construct a pH-sensitive long-cycle nanoliposome. This nanodrug delivery system, constructed using acid-sensitive biopolymers, can self-assemble in a medium into nanoparticles with an inner hydrophilic core and a hydrophobic bilayer. CTX, a water-soluble peptide, is encapsulated within the inner hydrophilic cavity and protected from enzymatic degradation.[43] When it enters the tumor site, the pH value starts to decrease gradually during cellular endocytosis. The acidic environment leads to the protonation of carboxylic acid groups in the lipid component of nanoparticles, which changes from hydrophobic to hydrophilic bonds, disrupting the balance between hydrophilic and hydrophobic bonds of

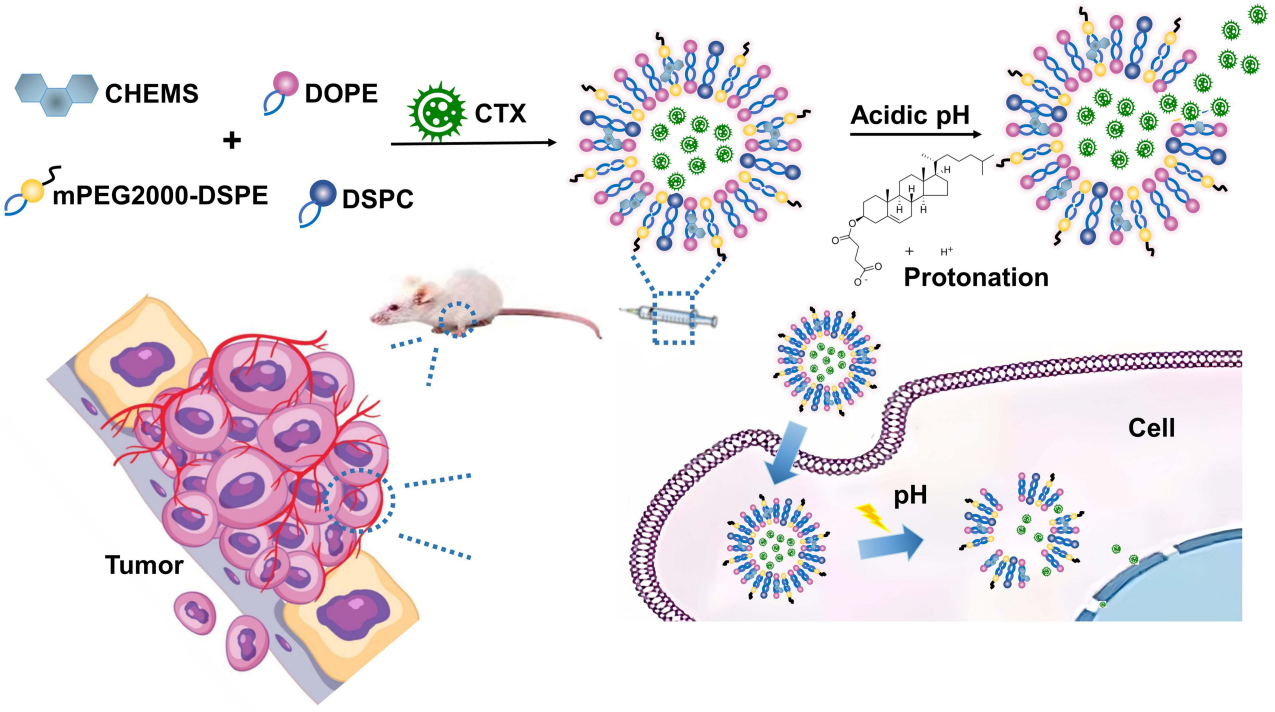

Figure 1 Self-assembly and release process of pH-sensitive nanoparticle loaded with CTX.

nanoparticles. This results in the membrane structure becoming a sparse hexagonal crystalline unstable structure, which eventually causes the destruction of the phospholipid bilayer structure,[44–46] thus allowing the targeted release of the drug within the lysosomes of tumor cells (Figure 1).

pH-sensitive long-circulating nanoliposomes were designed constructed with the following features: 1. CTX, a water-soluble drug, is encapsulated within the hydrophilic core of nanoliposome vesicles, and is protected from enzymatic degradation, improving protein stability and increasing bioavailability.[43,47] 2. With the enhanced permeability and retention (EPR) effect of nanoliposomes in tumor tissues, the drug is passively accumulated in tumor tissues, resulting in reduced distribution in normal tissues and organs, reducing the toxic side effects on surrounding cells and tissues.[48,49] 3. mPEG2000-DSPE as a modification material enhances the hydrophilicity of liposomes, reduces the interaction between plasma proteins and liposomes, reduces the possibility of rapid clearance by the reticuloendothelial system, prolongs the retention time of drugs in the circulatory system,[50,51] and overcomes the short half-life of protein drugs. 4. Using the characteristics of the acidic TME, the pH-sensitive response mechanisms of DOPE and CHEMS enhance the targeting of drugs, improve the uptake of drugs by tumor cells, and release drugs rapidly within tumor cells to increase drug concentrations, which together achieve enhanced targeted delivery and controlled release.[41]

Characterization and Stability of Cobra Venom Cytotoxin pH-Sensitive Liposomes

Several methods are available for preparing liposomes, each with unique characteristics. Based on the physicochemical properties of the encapsulated drug and laboratory conditions, we chose the thin film dispersion method to prepare cobra venom cytotoxin pH-sensitive liposomes (CTX@PSL).

The morphology of CTX@PSL was observed using transmission electron microscopy (TEM), and the liposomes were found to be irregularly spherical. By dynamic laser scattering (DLS) analysis, the average particle size of CTX@PSL was 127.92 ± 3.75 nm (Figure 2A and B). This is close to the pore size of the polycarbonate membrane (100 nm) used for extrusion, which enables the nanocarriers to evade phagocytosis by the reticuloendothelial system (RES), enter the tumor tissue through the vessel wall, accumulate in the tumor tissue, and achieve passive EPR effect-

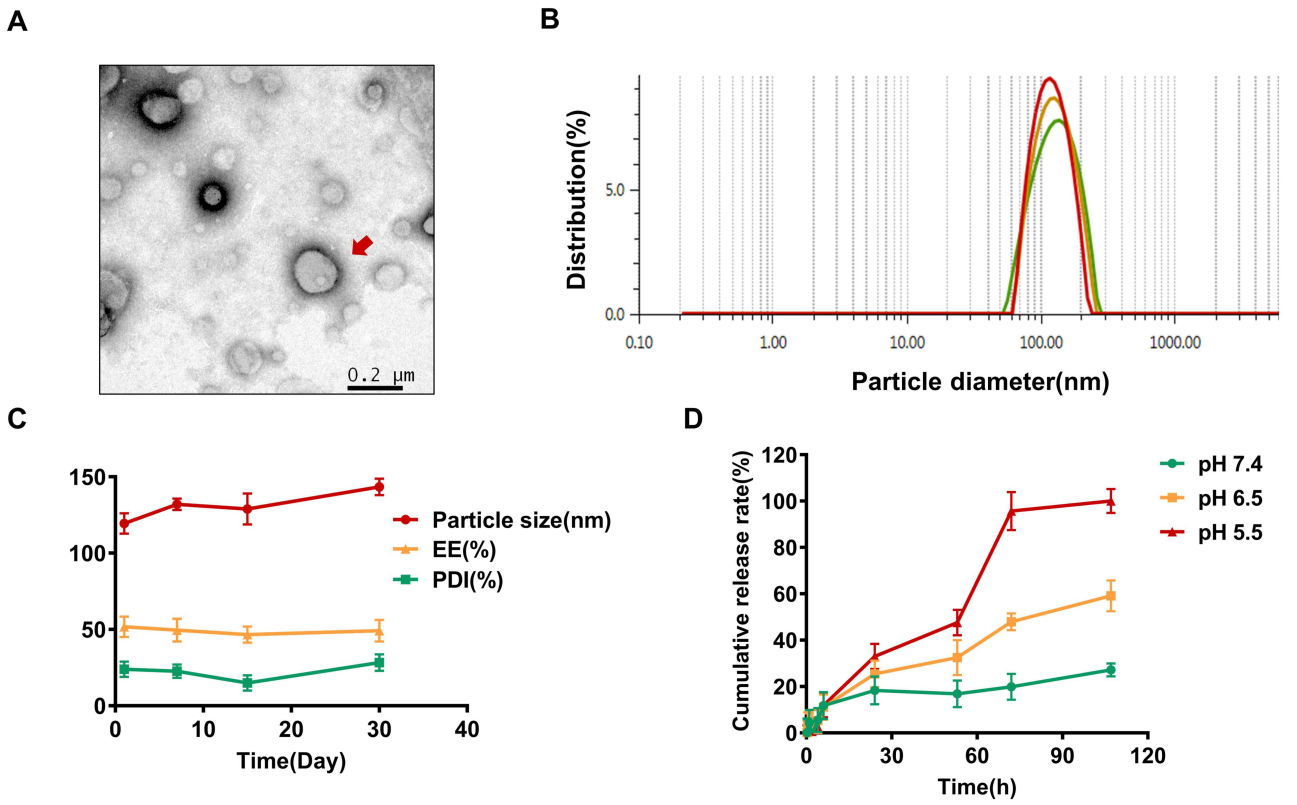

Figure 2 Characterization, Stability and drug release of CTX@PSL. (**A**) Morphology of CTX@PSL, the scale bar = 200 nm. (**B**) Particle size distribution of CTX@PSL. (**C**) CTX@PSL stability examination. (**D**) Effect of pH on the cumulative release of CTX@PSL in vitro.

targeting requirements.[52,53] The polydispersity index (PDI) was 15.00 ± 1.91%, indicating that the size distribution of nanoparticles was relatively homogeneous.[54,55] The average Zeta potential was −23.33 ± 0.67 mV, the relative pair negative charge is given by the amphiphilic stabilizer (CHEMS), and the electrostatic repulsion between particles in solution prevents aggregation and ensures stability.[44] The average encapsulation efficiency of CTX@PSL was 51.78 ± 1.63%, and the drug loading content was 8.84 ± 0.28%, which has potential for improvement, and more detailed optimization of liposome preparation conditions can be carried out subsequently.

Liposome stability is an important factor in clinical applications. The morphology, particle size, and surface charge of a nanocarrier affect its stability, resulting in aggregation and sedimentation. Liposomes prepared using DOPE and CHEMS appeared as creamy white suspensions without precipitation, flocculation, or delamination. These samples were stored at 4°C for 60 days and their stability was assessed based on particle size, polydispersity coefficient (PDI), and encapsulation efficiency (EE). Unfortunately, the long storage period had a damaging effect on the stability of liposomal drug delivery system, and the solution underwent settling and sticking after 60 days. However, the prepared CTX@PSL was stable after storage for up to 30 days. As shown in Figure 2C, the encapsulation efficiency of CTX@PSL did not change significantly with the extension of storage time, remaining at 46.55~51.72%, and no leakage was found. The hydrated particle size increased slightly, from 119.44 nm to 143.45 nm and PDI also increased, from 14.97 to 28.3% (Table S1). However, results from all stability criteria were within the acceptable range, and the solution did not show sticky sedimentation and turbidity.

Cytotoxin Release Profile

In vitro release assays were performed to examine the release behavior of CTX@PSL by simulating the pH of normal and tumor tissues in humans. Dialysis was used to assess the release of CTX from the nanocarriers by comparing the cumulative percentage release of drug-loaded nanoparticles in pH 7.4, pH 6.5, and pH 5.5 release media. The different

pH values correspond to the microenvironmental pH of the normal tissue, tumor tissue, and tumor cell lysosomes, respectively.

As shown in Figure 2D, the release behavior of CTX@PSL at different pH values were not significant in the first 12 h. The results indicated that CTX@PSL can stably exist under physiological conditions and even in the bloodstream in vivo for 12 hours.[38] Moreover, incorporation of PEG-modified liposomes increased their stability.[36,47] These properties can prevent premature drug release, prolong circulation in the bloodstream, 5 reduce exposure to free CTX outside the tumor tissue, and reduce toxicity. After 12 h, CTX@PSL was released fastest in a pH 5.5 medium. At pH 5.5, almost 95.69% of the CTX was released from the liposomes after 72 h. In contrast, only 27.17% of the CTX was released in the release medium at pH 7.4. This indicates that CTX@PSL can sustained and controlled release in tumor-acidic microenvironment. After reaching acidic tumor cells, the pH-sensitive chemical bonds on the liposomal membrane material are more easily protonated, disrupting the nanoparticle structure and releasing the drug. This enables targeted enrichment of CTX in tumor cells, reduces drug release within normal tissues, and increases therapeutic efficacy.[56]

Cell Uptake

We investigated whether this pH-responsive liposome, designed for the acidic TME, could promote drug uptake by B16-F10 cells. We labeled CTX with the vivo Tag™ 680XL Protein Labeling Kit to obtain a Dir@CTX to track its intracellular delivery. B16-F10 cells incubated with fluorescently labeled Dir@CTX and its nanoformulations were analyzed using flow cytometry. Cellular uptake was measured using the intracellular fluorescence intensity. Results showed that the intracellular fluorescence intensity from the fluorescently labeled protein vivo Tag™ 680XL became progressively stronger as the incubation time increased. The cellular uptake of Dir@CTX encapsulated by nanoliposomes increased significantly, and the pH-responsive liposomes, Dir@CTX@PSL, showed enhanced uptake compared to the regular liposomes, Dir@CTX@Lips (Figure 3). Cellular drug uptake increased up to 2.5 fold compared to that of free CTX. This is due to the artificial phospholipid materials DOPE and DSPC with alkaline amino end groups, which

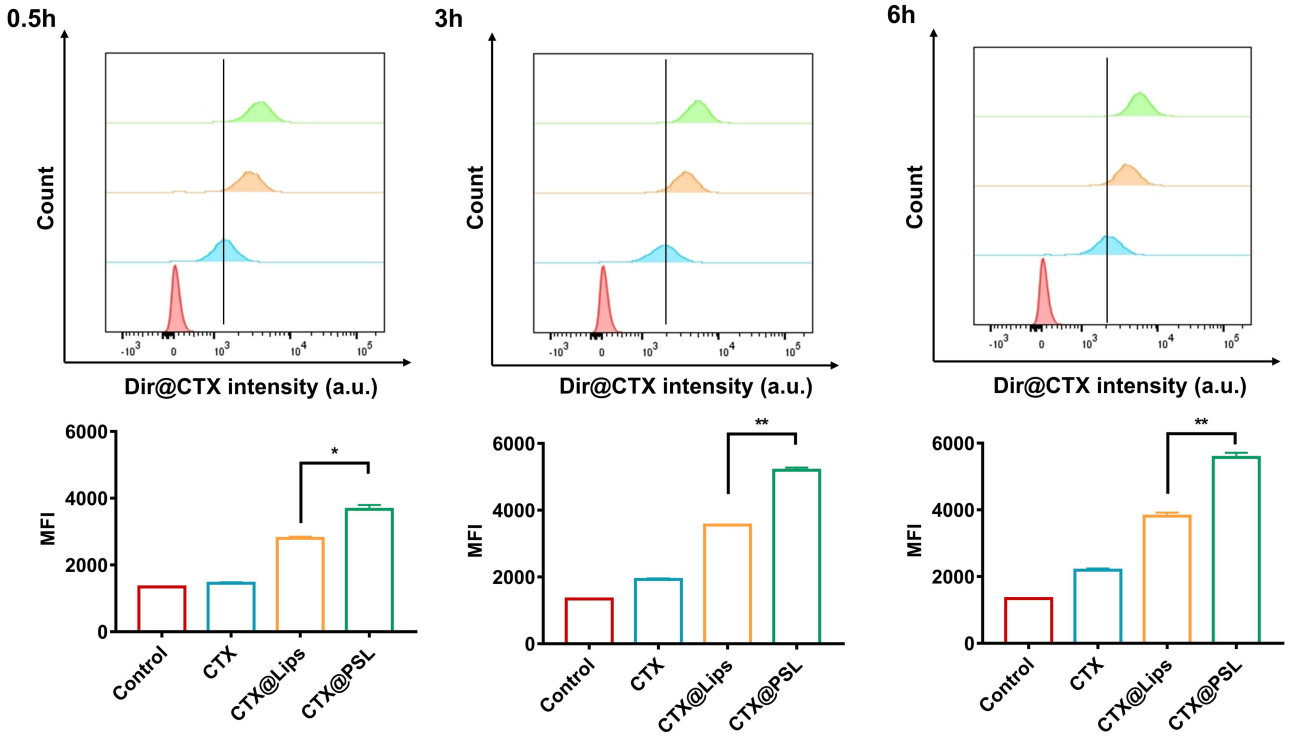

Figure 3 Cellular uptake efficacy of Dir@CTX loaded nanoparticles using flow cytometry, n = 3. All the data are presented as mean ± SD, *p<0.05, **p<0.01.

decrease the surface charge of Dir@CTX@PSL.[57,58] The acidic tumor environments leads to the protonation of carboxylic acid groups in the lipid component of Dir@CTX@PSL, which can enhance the affinity and uptake of CTX@PSL by tumor cells.

CTX@PSL Induced Apoptosis in B16-F10 Cells

Inhibiting cancer cell proliferation, halting cell cycle progression, and inducing apoptosis are the goals of chemotherapy in cancer treatment. Therefore, after detecting the inhibitory effect of CTX on proliferation using the MTT assay, we examined the apoptosis of B16-F10 cells by flow cytometry after Annexin V-FITC/PI double staining. The different quadrants in the images discriminate apoptotic, necrotic, and viable cells. CTX mainly induced late apoptosis,[11] and dead cells were simultaneously stained with Annexin V-FITC and PI. After incubation with B16-F10 cells for 24 h, the percentages of apoptosis induced by CTX@PSL, CTX@Lip, and free CTX were 71.78±1.70%, 56.2±3.04%, and 49.38±2.62%, respectively. The results showed that the apoptosis rate of CTX@PSL was significantly higher than that of CTX@Lips and free CTX ($p<0.01$) (Figure 4A and B). This indicates that CTX@PSL is more likely to enter the acidic B16-F10 tumor cells and promote apoptosis because of its pH-sensitive response to the acidic TME. This was consistent with the results of the MTT assay.

Proliferation Inhibition of B16-F10 Cells by CTX@PSL

Cytotoxins from cobra venom have been shown to have a killing effect on a variety of tumor cells and are promising antitumor agents.[59,60]

To investigate the effect of cytotoxins encapsulated in pH-sensitive nanoliposomes (CTX@PSL) on the proliferation of B16-F10 cells, we introduced normal liposomes without pH sensitivity (CTX@Lips) for comparison. B16-F10 cells were incubated with different concentrations of CTX@PSL, CTX@Lips, and free CTX under the same conditions for 24 h. It was found that in B16-F10 cells, both free CTX and its nanoformulations inhibited cell proliferation in a dose-dependent manner. The cytostatic effect increased with increasing drug concentrations (Figure 4C and Table 1). The IC_{50} values of CTX@PSL and CTX@Lips were 0.25 μg/mL and 0.48 μg/mL, respectively. Both exhibited stronger antitumor effects than free CTX (IC_{50} 0.54 μg/mL). Indeed, pH-sensitive liposomes can effectively deliver hydrophilic drugs to the cytoplasm.[33] Importantly, when encapsulated in pH-sensitive nanoliposomes, CTX can reach the lysosomes of tumor cells. This ability is expected to increase the efficacy and decrease toxicity when administered in vivo.

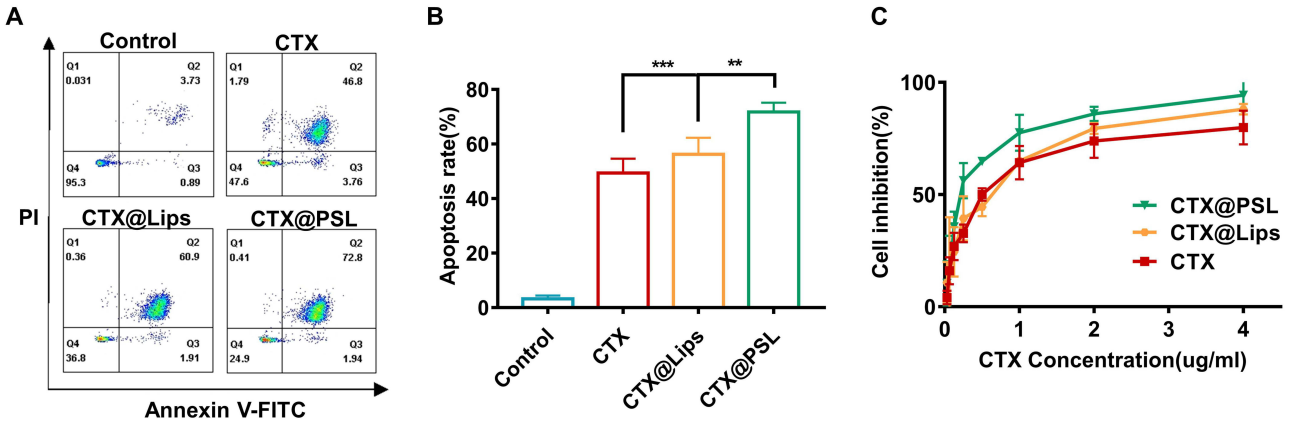

Figure 4 In vitro cytotoxicity assay. (**A** and **B**) FACS analysis of apoptosis induced by CTX in different liposome in B16-F10 cells (Mean ± SD, n = 4), **P < 0.01, ***P < 0.005. (**C**) Cellular inhibition of B16-F10 cells after 24h treatment (Mean ± SD, n = 6).

Table 1 Quantification of the Inhibitory Effect of Different Formulations of CTX on the Proliferation of B16-F10 Cells (Mean ± SD, n=6)

Concentration (μg/mL)	Cell Inhibition (%)		
	CTX	CTX@Lips	CTX@PSL
0.03	4.09 ± 3.04	10.76 ± 9.19	10.45 ± 9.86
0.06	16.08 ± 6.02	15.50 ± 4.44	14.48 ± 17.3
0.13	26.86 ± 6.07	24.34 ± 11.03	35.63 ± 6.72
0.25	32.67 ± 3.97	39.36 ± 9.82	56.23 ± 7.88
0.50	50.00 ± 2.77	44.43 ± 4.12	64.75 ± 1.46
1.00	64.19 ± 7.47	64.99 ± 0.96	77.55 ± 8.01
2.00	73.88 ± 4.27	79.45 ± 2.40	85.98 ± 3.19
4.00	79.88 ± 5.73	88.00 ± 6.54	94.25 ± 14.12
IC_{50} (95% CI)	0.54 (0.46~0.63)	0.48 (0.37~0.62)	0.25* (0.20~0.31)

Notes: *IC_{50} of CTX@PSL compared with CTX, *p<0.05.

In vivo Distribution

To visualize and quantify the distribution of CTX@PSL in vivo, a melanocytic tumor mouse model was established by subcutaneous inoculation of B16-F10 cells into ICR mice. When the tumor volume reached approximately 1000 mm^3, Dir@CTX@PSL and Dir@CTX were injected into the tail vein. Mice were sacrificed at different time points, and the main organs were collected for fluorescence imaging analysis. Fluorescence intensity data showed the cytotoxic content in each organ.

After intravenous injection, Dir@CTX was quickly distributed to the heart, liver, spleen, lung, kidney, and tumor tissues, and the fluorescence intensity in the liver and kidney was stronger, indicating hepatic metabolism and renal excretion. Data from previous laboratory studies of intravenous injection of CTX showed that the distribution half-life and elimination half-life in rabbits were 5.8 ± 0.6 min and 3.5 ± 0.2 h.[61] Owing to the rich blood flow in the liver and the important excretory role of the kidney, the drug concentrations were higher than those in other organs, which was consistent with the results of fluorescence imaging in mice.

At 0.5 h, the accumulation of Dir@CTX@PSL in the tumor tissues was significantly higher than that of free Dir@CTX ($p < 0.05$). Two hours after injection, the fluorescence intensity of Dir@CTX@PSL at the tumor site was about 6 fold higher than that of Dir@CTX, and the fluorescence signal was still evident after 6 h (Figures 5 and S1). The results of the fluorescence quantification analysis indicated that the constructed CTX@PSL nanoparticles could facilitate targeted enrichment in tumor tissues with an extended cycling pharmacokinetic profile.

However, considering that the pH value of the TME is closely related to the size of the tumor mass, ie, the stage of the tumor, the pH value in the TME and tumor cells will gradually decrease as the mass increases. Further studies are needed to investigate the correlation between tumor mass size and pH for a specific tumor species and the ability of pH-sensitive nanoformulations to target drug release to facilitate the selection of drug delivery timing and improve precision therapy.

Therapeutic Efficacy in a Melanoma Tumor Model

Tumor and Body Weight Reduction Measurements

The mouse B16-F10 tumor model was constructed using conventional methods. All subcutaneously grown melanocytic tumors in mice became tumorigenic, and the tumors emerged in approximately one week with a more regular spherical shape (Figure 6A).

The mice were randomly grouped after tumor formation. CTX and its nanoformulation were administered intraperitoneally at a dose of 0.6 mg/kg daily for 13 days. Surprisingly, both CTX@PSL and CTX exhibited superior inhibitory effects on tumor growth. The tumor weights of the treated mice were 0.47 ± 0.12 g and 0.98 ± 0.43 g, which were significantly lower than those of the untreated control group, 2.32 ± 0.89 g ($p<0.001$). Moreover, the tumor inhibition rate of CTX@PSL was higher at 79.78% compared to 53.93% for free CTX, showing a significant difference ($p<0.01$) (Figure 6B–D and Table 2). In vivo tumor suppression experiments in mice showed that the CTX@PSL group had the

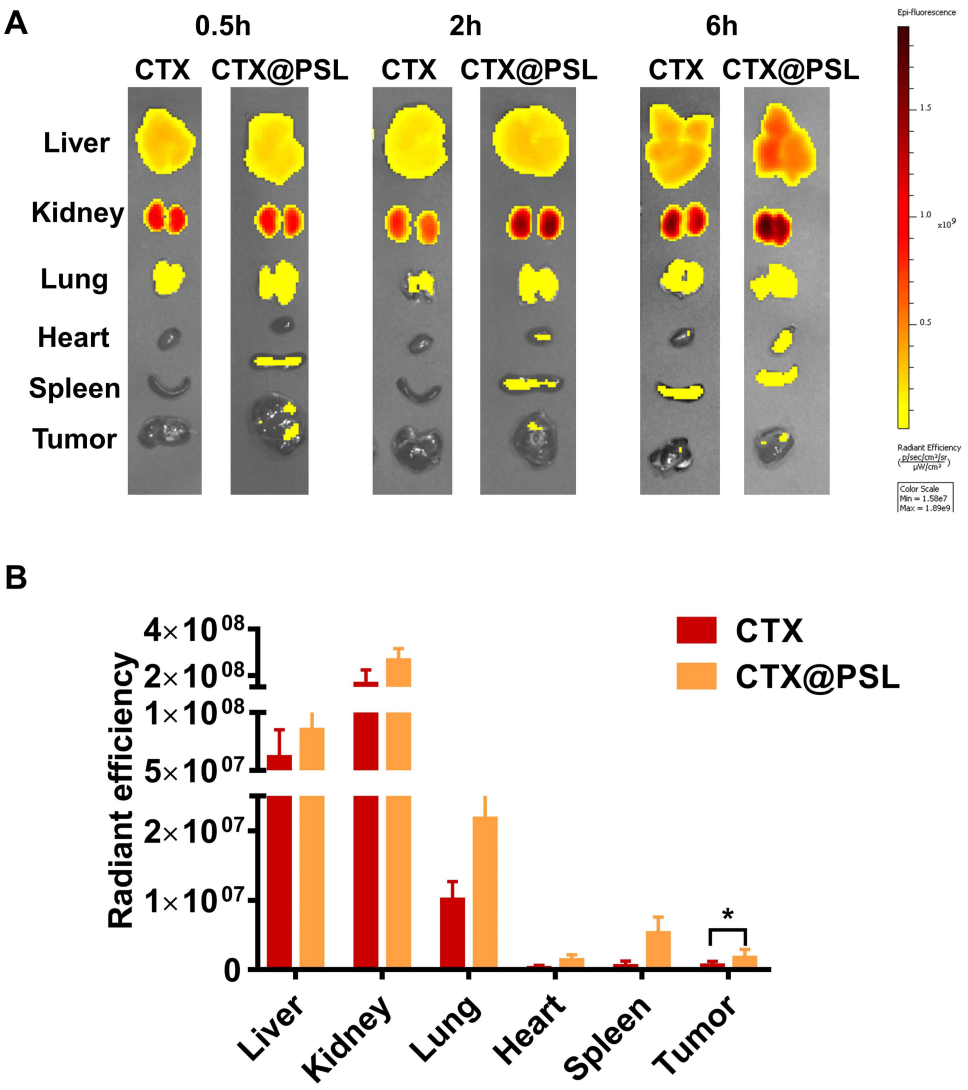

Figure 5 In vivo distribution. (**A**) Time-volume relationship of CTX@PSL in the targeting distribution of experimental melanoma growth in mice. (**B**) Distribution of CTX and CTX@PSL in tumor-bearing mice at 0.5h, *p < 0.05.

slowest tumor growth rate, smallest tumor mass, and highest tumor suppression rate compared to the control and CTX groups and had a superior tumor growth inhibition effect. Remarkably, the animals tolerated the lipid drug well, with no significant loss of body weight or increased mouse mortality after consecutive injections. However, we observed toxicity to cobra venom cytotoxin, with some mice showing depression, huddling, and decreased mobility after CTX injection, which resolved within a few hours. During the first week, the mice treated with CTX showed a weight loss of approximately 8% (Figure 6C). These results support that CTX@PSL enhanced the antitumor specificity of CTX through targeted delivery, thereby improving its efficacy and safety.

These results may be explained by the unique characteristics of these nanoformulations. CTX is confined within the liposome structure, which reduces the exposure of normal tissues to free CTX, decreasing drug toxicity. The EPR effect and pH-sensitive response of nanoparticles enable preferential accumulation in tumor lesions and increase the concentration of CTX in tumor cells, which leads to an enhanced antitumor effect.

Histopathology Assessment

Histological analyses of the different mouse organs were performed at the end of the treatment period. Because of the known uptake of liposomes by the liver, it is important to monitor the toxicity in these organs. In the CTX group,

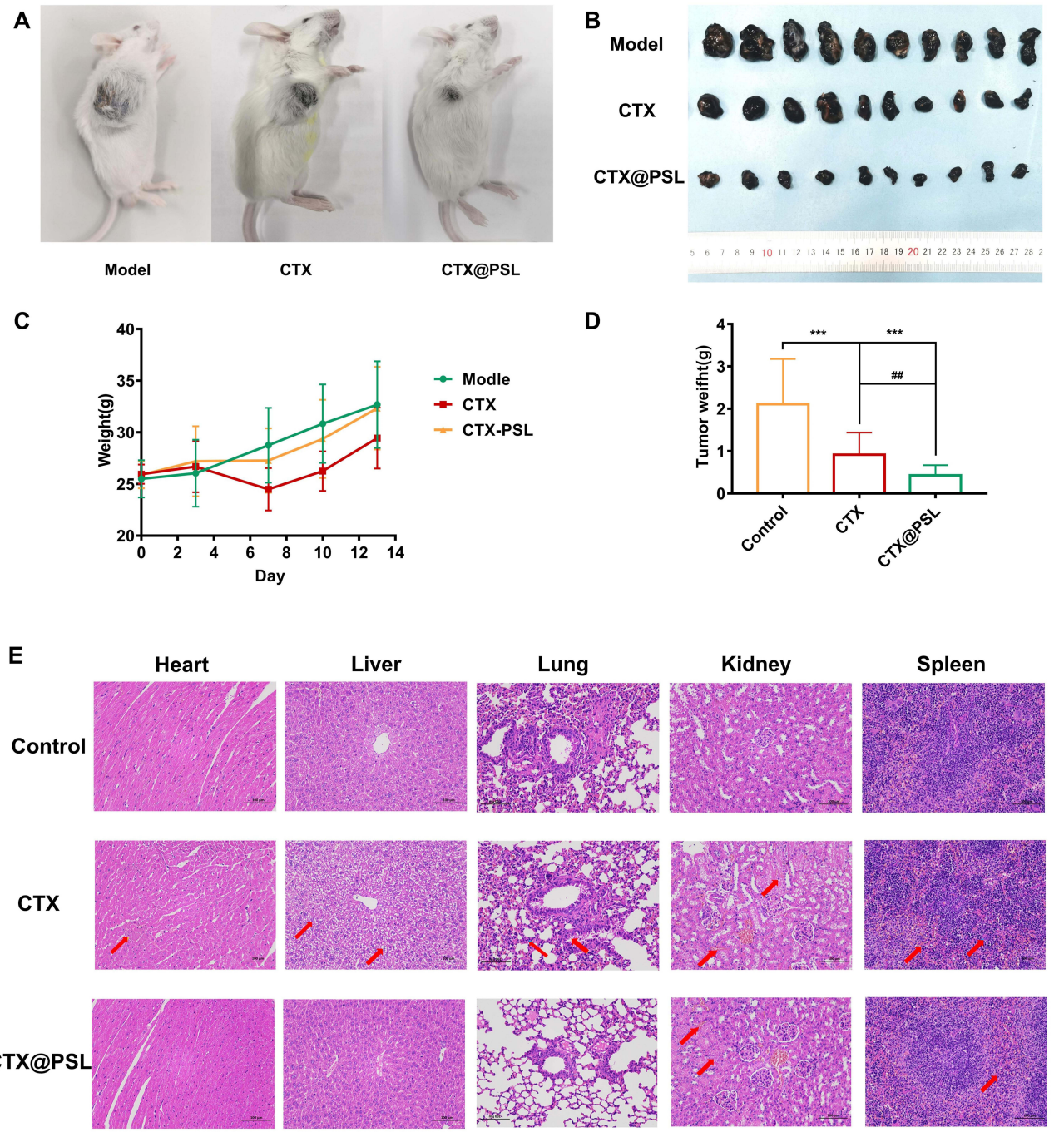

Figure 6 Therapeutic efficacy in a melanoma tumor model. (**A**) Melanoma growth in mice (some mice); (**B**) Melanoma masses exfoliated from mice; (**C**) Body weight gain curve of mice during treatment; (**D**) Inhibitory effect of CTX@PSL on the growth of melanoma in mice. All the data are presented as mean ± SD (n=10), $^{\#\#}p<0.01$, ***p<0.001; (**E**) Histological sections of ICR mice. Heart: red arrows indicate enhanced cytoplasmic eosinophilia and nuclear fixation of cardiomyocytes; Liver: red arrows indicate granular degeneration of hepatocytes and balloon-like degeneration; Lungs: red arrows indicate a small amount of eosinophilic granules visible in the bronchial lumen, mild thickening of the alveolar wall and inflammatory cell infiltration; Kidney: red arrows indicate tubular epithelial cell edema and interstitial stasis of the kidney; Spleen: red arrows indicate multinucleated giant cells visible in the red pulp, in addition to a few granulocytes. HE, scale bar = 100 μm.

extensive granular degeneration of hepatocytes with cytoplasmic sparing, light staining, and severe balloon-like degeneration was observed; however, at equivalent doses of CTX@PSL, the degree of degeneration was much lower (Figure 6E). Lung tissue sections from the CTX-treated group showed thickened alveolar walls and inflammatory cell infiltration in the visual field. The degree of alveolar wall thickening and inflammatory cell infiltration in the CTX@PSL group was relatively low compared to the CTX group.

Table 2 Inhibitory Effect of CTX@PSL on the Growth of Melanoma in Mice (Mean ± SD, n=10)

Group (mg/kg)	n	Body Weight (g)	Tumor Weight (g)	Inhibition Rate (%)
Control	10	32.19 ± 1.29	2.32 ± 0.89	–
CTX (0.6)	10	30.59 ± 1.67*	0.98 ± 0.43***	53.93 ± 18.72
CTX@PSL (0.6)	10	31.42 ± 1.05	0.47 ± 0.12***	79.78 ± 5.93$^{\#\#}$

Notes: Mouse body weight and tumor weight were the comparison between experimental group and model group, *p<0.05, **p<0.01, ***p<0.001; tumor inhibition rate was the comparison between CTX@PSL and CTX, $^{\#\#}$p<0.01.

Conclusion

In this study, we successfully designed and evaluated a novel pH-responsive liposome for the site-specific delivery and sustained release of CTX from *Cobra Venom*, which has 60–63 amino acid residues with a three-dimensional structure. Compared with free CTX, novel CTX-carrying pH-responsive liposome show that not only the biocompatibility is excellent, but also the stability is remarkable improved. The endogenous stimuli-responsive formulation of CTX, could take advantage of the lower pH of tumor cells to target the release drug, thereby increasing the uptake of CTX by tumor cells. However, whether the intracellular targets and effective mechanisms of free CTX or lipids delivery systems are altered after entering target cells remains to be further explored, and we will conduct a series of studies on this in the future. Additionally, CTX@PSL significantly prolongs drug accumulation and retention time in tumor lesions, leading to a significant improvement in antitumor efficacy while reducing its toxic side effects. These encouraging results demonstrate that the pH-sensitive liposome have excellent encapsulation efficiency and drug loading capacity for CTX. It's a promising strategy to enhance delivery efficiency and local drug concentration, and reduce drug dosage, which provides a potential clinical translation strategy for the treatment of malignant melanoma.

Ethics Approval and Consent to Participate

All the animal experiments were approved by the Experimental Animal Center of Fujian Medical University. Animal experiments were carried out in compliance with the Guide for the Animals Care and Ethics Committee of Fujian Medical University (Certificate number: IACUC FJMU 2022-0416).

Acknowledgments

This research was funded by the Natural Science Foundation of Fujian province (2020J01631), Joint Funds for the innovation of science and Technology of Fujian province (2018Y9076), Fujian Medical University Startup Fund for Scientific Research (2020QH1254). We acknowledge the Fujian Medical University Ethics Committee for their kind guidance in the animal experiments and the Public Technology Service Center of Fujian Medical University.

Disclosure

The authors declare no conflicts of interest.

References

1. Jenkins RW, Fisher DE. Treatment of advanced melanoma in 2020 and beyond. *J Invest Dermatol*. 2021;141(1):23–31. doi:10.1016/j.jid.2020.03.943
2. Arnold M, Singh D, Laversanne M, et al. Global burden of cutaneous melanoma in 2020 and projections to 2040. *JAMA Dermatol*. 2022;158(5):495–503. doi:10.1001/jamadermatol.2022.0160
3. Marin-Bejar O, Rogiers A, Dewaele M, et al. Evolutionary predictability of genetic versus nongenetic resistance to anticancer drugs in melanoma. *Cancer Cell*. 2021;39(8):1135–1149.e1138. doi:10.1016/j.ccell.2021.05.015
4. Czarnecka AM, Bartnik E, Fiedorowicz M, Rutkowski P. Targeted therapy in melanoma and mechanisms of resistance. *Int J Mol Sci*. 2020;21(13):4576. doi:10.3390/ijms21134576
5. Liu CC, Wu CJ, Chou TY, et al. Development of a monoclonal scFv against cytotoxin to neutralize cytolytic activity induced by naja atra venom on myoblast C2C12 cells. *Toxins*. 2022;14(7):459. doi:10.3390/toxins14070459
6. Beraldo E, Coelho GR, Sciani JM, Pimenta DC. Proteomic characterization of Naja mandalayensis venom. *J Venom Anim Toxins Incl Trop Dis*. 2021;27:e20200125 doi:10.1590/1678-9199-JVATITD-2020-0125
7. Dubovskii PV, Efremov RG. The role of hydrophobic /hydrophilic balance in the activity of structurally flexible vs. rigid cytolytic polypeptides and analogs developed on their basis. *Expert Rev Proteom*. 2018;15(11):873–886. doi:10.1080/14789450.2018.1537786

8. Dubovskii PV, Dubova KM, Bourenkov G, et al. Variability in the spatial structure of the central loop in cobra cytotoxins revealed by X-ray analysis and molecular modeling. *Toxins*. 2022;14(2):149. doi:10.3390/toxins14020149
9. Li F, Shrivastava IH, Hanlon P, Dagda RK, Gasanoff ES. Molecular mechanism by which cobra venom cardiotoxins interact with the outer mitochondrial membrane. *Toxins*. 2020;12(7):425. doi:10.3390/toxins12070425
10. Hiu JJ, Yap MKK. The effects of Naja sumatrana venom cytotoxin, sumaCTX on alteration of the secretome in MCF-7 breast cancer cells following membrane permeabilization. *Int J Biol Macromol*. 2021;184:776–786. doi:10.1016/j.ijbiomac.2021.06.145
11. Liu Y, Ming W, Wang Y, et al. Cytotoxin 1 from Naja atra Cantor venom induced necroptosis of leukemia cells. *Toxicon*. 2019;165:110–115. doi:10.1016/j.toxicon.2019.04.012
12. Abdel-Ghani LM, Rahmy TR, Tawfik MM, et al. Cytotoxicity of Nubein6.8 peptide isolated from the snake venom of Naja nubiae on melanoma and ovarian carcinoma cell lines. *Toxicon*. 2019;168:22–31. doi:10.1016/j.toxicon.2019.06.220
13. Derakhshani A, Silvestris N, Hajiasgharzadeh K, et al. Expression and characterization of a novel recombinant cytotoxin II from Naja naja oxiana venom: a potential treatment for breast cancer. *Int J Biol Macromol*. 2020;162:1283–1292. doi:10.1016/j.ijbiomac.2020.06.130
14. Chong HP, Tan KY, Tan CH. Cytotoxicity of snake venoms and cytotoxins from two southeast asian cobras (Naja sumatrana, Naja kaouthia): exploration of anticancer potential, selectivity, and cell death mechanism. *Front Mol Biosci*. 2020;7:583587. doi:10.3389/fmolb.2020.583587
15. Wong KY, Tan KY, Tan NH, Tan CH. A neurotoxic snake venom without phospholipase A(2): proteomics and cross-neutralization of the venom from senegalese cobra, naja senegalensis (Subgenus: uraeus). *Toxins*. 2021;13(1):60. doi:10.3390/toxins13010060
16. Derakhshani A, Silvestris N, Hemmat N, et al. Targeting TGF-β-mediated SMAD signaling pathway via novel recombinant cytotoxin II: a potent protein from naja naja oxiana venom in melanoma. *Molecules*. 2020;25(21):5148. doi:10.3390/molecules25215148
17. Chen B, Wang X, Zhang Y, et al. Improved solubility, dissolution rate, and oral bioavailability of main biflavonoids from Selaginella doederleinii extract by amorphous solid dispersion. *Drug Delivery*. 2020;27(1):309–322. doi:10.1080/10717544.2020.1716876
18. Fei B, Mo Z, Yang J, Wang Z, Li S. Nanodrugs reprogram cancer-associated fibroblasts and normalize tumor vasculatures for sequentially enhancing photodynamic therapy of hepatocellular carcinoma. *Int J Nanomed*. 2023;18:6379–6391. doi:10.2147/IJN.S429884
19. Li Q, Zhou Y, He W, et al. Platelet-armored nanoplatform to harmonize janus-faced IFN-γ against tumor recurrence and metastasis. *J Control Release*. 2021;338:33–45. doi:10.1016/j.jconrel.2021.08.020
20. Lin Y, Chen X, Yu C, et al. Radiotherapy-mediated redox homeostasis-controllable nanomedicine for enhanced ferroptosis sensitivity in tumor therapy. *Acta Biomater*. 2023;159:300–311. doi:10.1016/j.actbio.2023.01.022
21. Gong L, Lu Y, Wang J, et al. Cocktail hepatocarcinoma therapy by a super-assembled nano-pill targeting XPO1 and ATR synergistically. *J Pharm Anal*. 2023;13(6):603–615. doi:10.1016/j.jpha.2023.04.017
22. Chen B, Wang X, Lin D, et al. Proliposomes for oral delivery of total biflavonoids extract from Selaginella doederleinii: formulation development, optimization, and in vitro-in vivo characterization. *Int J Nanomed*. 2019;14:6691–6706. doi:10.2147/IJN.S214686
23. Bhattarai RS, Bariwal J, Kumar V, et al. pH-sensitive nanomedicine of novel tubulin polymerization inhibitor for lung metastatic melanoma. *J Control Release*. 2022;350:569–583. doi:10.1016/j.jconrel.2022.08.023
24. Huang S, Zhang Y, Wang L, et al. Improved melanoma suppression with target-delivered TRAIL and Paclitaxel by a multifunctional nanocarrier. *J Control Release*. 2020;325:10–24. doi:10.1016/j.jconrel.2020.03.049
25. Alrbyawi H, Poudel I, Annaji M, et al. pH-sensitive liposomes for enhanced cellular uptake and cytotoxicity of daunorubicin in melanoma (B16-BL6) cell lines. *Pharmaceutics*. 2022;14(6):1128. doi:10.3390/pharmaceutics14061128
26. Chen B, Zheng K, Fang S, et al. B7H3 targeting gold nanocage pH-sensitive conjugates for precise and synergistic chemo-photothermal therapy against NSCLC. *J Nanobiotechnol*. 2023;21(1):378. doi:10.1186/s12951-023-02078-9
27. Majumder J, Minko T. Multifunctional and stimuli-responsive nanocarriers for targeted therapeutic delivery. *Expert Opin Drug Deliv*. 2021;18 (2):205–227. doi:10.1080/17425247.2021.1828339
28. Deepak KGK, Vempati R, Nagaraju GP, et al. Tumor microenvironment: challenges and opportunities in targeting metastasis of triple negative breast cancer. *Pharmacol Res*. 2020;153:104683 doi:10.1016/j.phrs.2020.104683
29. Zhang C, Shen H, Yang T, et al. A single-cell analysis reveals tumor heterogeneity and immune environment of acral melanoma. *Nat Commun*. 2022;13(1):7250. doi:10.1038/s41467-022-34877-3
30. Karras P, Bordeu I, Pozniak J, et al. A cellular hierarchy in melanoma uncouples growth and metastasis. *Nature*. 2022;610(7930):190–198. doi:10.1038/s41586-022-05242-7
31. Vaupel P, Multhoff G. Revisiting the Warburg effect: historical dogma versus current understanding. *J Physiol*. 2021;599(6):1745–1757. doi:10.1113/JP278810
32. Peng S, Xiao F, Chen M, Gao H. Tumor-microenvironment-responsive nanomedicine for enhanced cancer immunotherapy. *Adv Sci*. 2022;9(1): e2103836. doi:10.1002/advs.202103836
33. Li R, Xie Y. Nanodrug delivery systems for targeting the endogenous tumor microenvironment and simultaneously overcoming multidrug resistance properties. *J Control Release*. 2017;251:49–67. doi:10.1016/j.jconrel.2017.02.020
34. Imtiyaz Z, He J, Leng Q, Agrawal AK, Mixson AJ. pH-sensitive targeting of tumors with chemotherapy-laden nanoparticles: progress and challenges. *Pharmaceutics*. 2022;14(11):2427. doi:10.3390/pharmaceutics14112427
35. Pontrelli G, Toniolo G, McGinty S, Peri D, Succi S, Chatgilialoglu C. Mathematical modelling of drug delivery from pH-responsive nanocontainers. *Comput Biol Med*. 2021;131:104238. doi:10.1016/j.compbiomed.2021.104238
36. Kim KS, Kwag DS, Hwang HS, Lee ES, Bae YH. Immense insulin intestinal uptake and lymphatic transport using bile acid conjugated partially uncapped liposome. *Mol Pharm*. 2018;15(10):4756–4763. doi:10.1021/acs.molpharmaceut.8b00708
37. Kabil MF, Mahmoud MY, Bakr AF, Zaafar D, El-Sherbiny IM. Switching indication of PEGylated lipid nanocapsules-loaded with rolapitant and deferasirox against breast cancer: enhanced in-vitro and in-vivo cytotoxicity. *Life Sci*. 2022;305:120731. doi:10.1016/j.lfs.2022.120731
38. Bozzuto G, Molinari A. Liposomes as nanomedical devices. *Int J Nanomed*. 2015;10:975–999. doi:10.2147/IJN.S68861
39. Hiu JJ, Yap MKK. The myth of cobra venom cytotoxin: more than just direct cytolytic actions. *Toxicon X*. 2022;14:100123. doi:10.1016/j.toxcx.2022.100123
40. Wu M, Ming W, Tang Y, Zhou S, Kong T, Dong W. The anticancer effect of cytotoxin 1 from Naja atra Cantor venom is mediated by a lysosomal cell death pathway involving lysosomal membrane permeabilization and cathepsin B release. *Am J Chin Med*. 2013;41(3):643–663. doi:10.1142/S0192415X13500456

41. Pang X, Jiang Y, Xiao Q, Leung AW, Hua H, Xu C. pH-responsive polymer-drug conjugates: design and progress. *J Control Release*. 2016;222:116–129. doi:10.1016/j.jconrel.2015.12.024
42. Gannimani R, Walvekar P, Naidu VR, Aminabhavi TM, Govender T. Acetal containing polymers as pH-responsive nano-drug delivery systems. *J Control Release*. 2020;328:736–761. doi:10.1016/j.jconrel.2020.09.044
43. Rezaei N, Mehrnejad F, Vaezi Z, Sedghi M, Asghari SM, Naderi-Manesh H. Encapsulation of an endostatin peptide in liposomes: stability, release, and cytotoxicity study. *Colloids Surf B Biointerfaces*. 2020;185:110552. doi:10.1016/j.colsurfb.2019.110552
44. Ducat E, Deprez J, Gillet A, et al. Nuclear delivery of a therapeutic peptide by long circulating pH-sensitive liposomes: benefits over classical vesicles. *Int J Pharm*. 2011;420(2):319–332. doi:10.1016/j.ijpharm.2011.08.034
45. Sethuraman V, Janakiraman K, Krishnaswami V, Kandasamy R. Recent progress in stimuli-responsive intelligent nano scale drug delivery systems: a special focus towards pH-sensitive systems. *Curr Drug Targets*. 2021;22(8):947–966. doi:10.2174/1389450122999210128180058
46. Zhuo S, Zhang F, Yu J, Zhang X, Yang G, Liu X. pH-sensitive biomaterials for drug delivery. *Molecules*. 2020;25(23):5649. doi:10.3390/molecules25235649
47. Meng Y, Chen J, Liu Y, et al. A highly efficient protein Corona-based proteomic analysis strategy for the discovery of pharmacodynamic biomarkers. *J Pharm Anal*. 2022;12(6):879–888. doi:10.1016/j.jpha.2022.07.002
48. Han W, Shi L, Xie B, et al. Supramolecular engineering of molecular inhibitors in an adaptive cytotoxic nanoparticle for synergistic cancer therapy. *ACS Appl Mater Interfaces*. 2020;12(1):1707–1720. doi:10.1021/acsami.9b20178
49. Strijkers GJ, Kluza E, Van Tilborg GA, et al. Paramagnetic and fluorescent liposomes for target-specific imaging and therapy of tumor angiogenesis. *Angiogenesis*. 2010;13(2):161–173. doi:10.1007/s10456-010-9165-1
50. Lozano N, Al-Ahmady ZS, Beziere NS, Ntziachristos V, Kostarelos K. Monoclonal antibody-targeted PEGylated liposome-ICG encapsulating doxorubicin as a potential theranostic agent. *Int J Pharm*. 2015;482(1–2):2–10. doi:10.1016/j.ijpharm.2014.10.045
51. Wang Y, Zhang S, Benoit DSW. Degradable poly(ethylene glycol) (PEG)-based hydrogels for spatiotemporal control of siRNA/nanoparticle delivery. *J Control Release*. 2018;287:58–66. doi:10.1016/j.jconrel.2018.08.002
52. Fang J, Nakamura H, Maeda H. The EPR effect: unique features of tumor blood vessels for drug delivery, factors involved, and limitations and augmentation of the effect. *Adv Drug Deliv Rev*. 2011;63(3):136–151. doi:10.1016/j.addr.2010.04.009
53. Nie D, Liu C, Yu M, Jiang X, Wang N, Gan Y. Elasticity regulates nanomaterial transport as delivery vehicles: design, characterization, mechanisms and state of the art. *Biomaterials*. 2022;291:121879. doi:10.1016/j.biomaterials.2022.121879
54. Al-Joufi FA, Salem-Bekhit MM, Taha EI, et al. Enhancing ocular bioavailability of ciprofloxacin using colloidal lipid-based carrier for the management of post-surgical infection. *Molecules*. 2022;27(3):733. doi:10.3390/molecules27030733
55. Perez-Potti A, Rodríguez-Pérez M, Polo E, Pelaz B, Del Pino P. Nanoparticle-based immunotherapeutics: from the properties of nanocores to the differential effects of administration routes. *Adv Drug Deliv Rev*. 2023;197:114829 doi:10.1016/j.addr.2023.114829
56. Shi L, Wang Y, Wang Q, et al. Transforming a toxic drug into an efficacious nanomedicine using a lipoprodrug strategy for the treatment of patient-derived melanoma xenografts. *J Control Release*. 2020;324:289–302. doi:10.1016/j.jconrel.2020.05.025
57. Gu Z, Da Silva CG, Hao Y, et al. Effective combination of liposome-targeted chemotherapy and PD-L1 blockade of murine colon cancer. *J Control Release*. 2023;353:490–506. doi:10.1016/j.jconrel.2022.11.049
58. Van Broekhoven CL, Altin JG. A novel system for convenient detection of low-affinity receptor-ligand interactions: chelator-lipid liposomes engrafted with recombinant CD4 bind to cells expressing MHC class II. *Immunol Cell Biol*. 2001;79(3):274–284. doi:10.1046/j.1440-1711.2001.01010.x
59. Chen KC, Kao PH, Lin SR, Chang LS. The mechanism of cytotoxicity by Naja naja atra cardiotoxin 3 is physically distant from its membrane-damaging effect. *Toxicon*. 2007;50(6):816–824. doi:10.1016/j.toxicon.2007.06.011
60. Wang Y, Lin LW, Chen ZK, et al. Effects of intratumoral injection of microspheres containing cobra venom cytotoxin on transplanted human hepatoma in nude mice. *Zhong Xi Yi Jie He Xue Bao*. 2009;7(9):836–841. doi:10.3736/jcim20090908
61. Guo MP, Wang QC, Liu GF. Pharmacokinetics of cytotoxin from Chinese cobra (Naja naja atra) venom. *Toxicon*. 1993;31(3):339–343. doi:10.1016/0041-0101(93)90151-8